

## Structure of the $N = 50$ As, Ge, Ga nuclei

E. Sahin<sup>a,b,\*</sup>, G. de Angelis<sup>a</sup>, G. Duchene<sup>c</sup>, T. Faul<sup>c</sup>, A. Gadea<sup>a,d</sup>,  
A.F. Lisetskiy<sup>e</sup>, D. Ackermann<sup>f</sup>, A. Algora<sup>d,g</sup>, S. Aydin<sup>h,i</sup>, F. Azaiez<sup>j</sup>,  
D. Bazzacco<sup>i</sup>, G. Benzoni<sup>k</sup>, M. Bostan<sup>l</sup>, T. Byrski<sup>c</sup>, I. Celikovic<sup>m</sup>,  
R. Chapman<sup>n</sup>, L. Corradi<sup>a</sup>, S. Courtin<sup>c</sup>, D. Curien<sup>c</sup>, U. Datta Pramanik<sup>o</sup>,  
F. Didierjean<sup>p</sup>, O. Dorvaux<sup>c</sup>, M.N. Erduran<sup>q</sup>, S. Erturk<sup>r</sup>, E. Farnea<sup>i</sup>,  
E. Fioretto<sup>a</sup>, G. de France<sup>s</sup>, S. Franchoo<sup>j</sup>, B. Gall<sup>c</sup>, A. Gottardo<sup>a,i</sup>,  
B. Guiot<sup>a</sup>, F. Haas<sup>c</sup>, F. Ibrahim<sup>j</sup>, E. Ince<sup>t</sup>, A. Khouaja<sup>c</sup>, A. Kusoglu<sup>l</sup>,  
G. La Rana<sup>u</sup>, M. Labiche<sup>v</sup>, D. Lebhertz<sup>c</sup>, S. Lenzi<sup>i</sup>, S. Leoni<sup>k</sup>,  
S. Lunardi<sup>i</sup>, P. Mason<sup>i</sup>, D. Mengoni<sup>i,n</sup>, C. Michelagnoli<sup>i</sup>, V. Modamio<sup>a</sup>,  
G. Montagnoli<sup>i</sup>, D. Montanari<sup>i</sup>, R. Moro<sup>u</sup>, B. Mouginit<sup>j</sup>, D.R. Napoli<sup>a</sup>,  
D. O'Donnell<sup>n</sup>, J.R.B. Oliveira<sup>w</sup>, J. Ollier<sup>n</sup>, R. Orlandi<sup>n</sup>, G. Pollarolo<sup>x</sup>,  
F. Recchia<sup>i</sup>, J. Robin<sup>c</sup>, M.-D. Salsac<sup>y</sup>, F. Scarlassara<sup>i</sup>, R.P. Singh<sup>z</sup>,  
R. Silvestri<sup>a</sup>, J.F. Smith<sup>n</sup>, I. Stefan<sup>j</sup>, A.M. Stefanini<sup>a</sup>, K. Subotic<sup>m</sup>,  
S. Szilner<sup>aa</sup>, D. Tonev<sup>ab</sup>, D.A. Torres<sup>n</sup>, M. Trotta<sup>u</sup>, P. Ujic<sup>m</sup>, C. Ur<sup>i</sup>,  
J.J. Valiente-Dobón<sup>a</sup>, D. Verney<sup>j</sup>, M. Yalcinkaya<sup>l</sup>, P.T. Wady<sup>n</sup>,  
K.T. Wiedemann<sup>w</sup>, K. Zuber<sup>ac</sup>

<sup>a</sup> Laboratori Nazionali di Legnaro dell'INFN, Legnaro, Italy

<sup>b</sup> Department of Physics, University of Oslo, NO-0316 Oslo, Norway

<sup>c</sup> IPHC, IN2P3/CNRS et Université Louis Pasteur, Strasbourg, France

<sup>d</sup> Instituto de Física Corpuscular, CSIC – Universidad de Valencia, Valencia, Spain

<sup>e</sup> Department of Physics, University of Arizona, Tucson, AZ, USA

<sup>f</sup> Helmholtzzentrum für Schwerionenforschung (GSI), Darmstadt, Germany

<sup>g</sup> Institute of Nuclear Research, Debrecen, Hungary

<sup>h</sup> Department of Physics, University of Aksaray, Aksaray, Turkey

<sup>i</sup> INFN Sezione di Padova and Dipartimento di Fisica, Università di Padova, Padova, Italy

<sup>j</sup> IPNO, IN2P3/CNRS et Université Paris-Sud, Orsay, France

<sup>k</sup> INFN Sezione di Milano and Dipartimento di Fisica, Università di Milano, Milano, Italy

<sup>l</sup> Department of Physics, Istanbul University, Istanbul, Turkey

<sup>m</sup> Vinca Institute of Nuclear Sciences, Belgrade, Serbia

<sup>n</sup> University of the West of Scotland, Paisley, United Kingdom

<sup>o</sup> Saha Institute of Nuclear Physics, Kolkata, India

<sup>p</sup> Institut Pluridisciplinaire Hubert Curien, Strasbourg, France

<sup>q</sup> Istanbul Sabahattin Zaim University, Istanbul, Turkey

<sup>r</sup> Department of Physics, Nigde University, Nigde, Turkey

<sup>s</sup> GANIL, Caen, France

<sup>t</sup> Istanbul University, Hasan Ali Yucel Education Faculty, Science Education, Istanbul, Turkey

<sup>u</sup> INFN Sezione di Napoli and Dipartimento di Scienze Fisiche, Università di Napoli, Napoli, Italy

<sup>v</sup> STFC, Daresbury Laboratory, Daresbury Warrington, United Kingdom

<sup>w</sup> University of São Paulo, São Paulo, Brazil

<sup>x</sup> Dipartimento di Fisica Teorica, Università di Torino, Via Pietro Giuria I, Torino, Italy

<sup>y</sup> CEA Saclay, IRFU/SPhN, France

<sup>z</sup> Inter-University Accelerator Center, New Delhi 67, India

<sup>aa</sup> Ruđer Bošković Institute, HR-10001 Zagreb, Croatia

<sup>ab</sup> Institute for Nuclear Research and Nuclear Energy, BAS, Sofia, Bulgaria

<sup>ac</sup> Institute of Nuclear Physics, Krakow, Poland

Received 27 April 2012; received in revised form 21 July 2012; accepted 6 August 2012

Available online 6 September 2012

---

## Abstract

The level structures of the  $N = 50$   $^{83}\text{As}$ ,  $^{82}\text{Ge}$ , and  $^{81}\text{Ga}$  isotones have been investigated by means of multi-nucleon transfer reactions. A first experiment was performed with the CLARA–PRISMA setup to identify these nuclei. A second experiment was carried out with the GASP array in order to deduce the  $\gamma$ -ray coincidence information. The results obtained on the high-spin states of such nuclei are used to test the stability of the  $N = 50$  shell closure in the region of  $^{78}\text{Ni}$  ( $Z = 28$ ). The comparison of the experimental level schemes with the shell-model calculations yields an  $N = 50$  energy gap value of 4.7(3) MeV at  $Z = 28$ . This value, in a good agreement with the prediction of the finite-range liquid-drop model as well as with the recent large-scale shell model calculations, does not support a weakening of the  $N = 50$  shell gap down to  $Z = 28$ .

© 2012 Elsevier B.V. All rights reserved.

**Keywords:** NUCLEAR REACTIONS  $^{238}\text{U}(^{82}\text{Se}, ^{81}\text{Ga}), (^{82}\text{Se}, ^{82}\text{Ge}), (^{82}\text{Se}, ^{83}\text{As}), E = 515$  MeV; measured  $E_\gamma, I_\gamma(\theta)$ ,  $\gamma\gamma$ -coin, reaction fragments, (fragment) $\gamma$ -coin using PRISMA magnetic spectrometer,  $\gamma$  after deexcitation using Ge Compton-suppressed detectors of CLARA array, thin and thick target; deduced  $\sigma(\theta)$ , levels,  $J, \pi$ ; calculated levels,  $J, \pi$  using shell model

---

## 1. Introduction

Magic numbers are a key feature in finite Fermion systems since they are strongly related to the underlying mean field. Their existence and stability suggested the presence of closed-shell configurations and led to the development of the Shell Model in atomic nuclei. Recently, theoretical predictions [1–3] and experimental results have indicated that magic numbers evolve along isotopic/isotonic chains throughout the nuclear chart, exhibiting a more localized applicability. Changes in the size of the shell gaps are expected to happen especially in neutron-rich, loosely-bound systems due to the combined effects of the density dependence of the residual interaction and in particular of the tensor interaction [3], the many-body correlations (such as pairing) involving weakly-bound and unbound nucleons, and the fact that at the neutron drip-line the nucleus cannot be represented anymore as a closed quantum system [4]. The evolution of

---

\* Corresponding author.

E-mail address: eda.sahin@lnl.infn.it (E. Sahin).

magic numbers and the breakdown of the shell gaps, found along the line of stability, have been predicted and observed in different mass regions [5]. The modification of the strength of shell effects away from stability also has an astrophysical importance. Since shell effects are force-dependent, the experimental determination of the shell gaps far from stability allows various forces, and therefore different mass formulae for astrophysics, to be probed. Considerable theoretical effort has improved the reliability of nuclear mass formulas using different microscopic forces [6]. Currently, the size of the  $N = 50$  shell gap with increasing neutron-to-proton ratio is of great interest due to its impact on nuclear structure and astrophysical properties. It is situated between the  $g_{9/2}$  and  $d_{5/2}$  orbits. The largest value for this gap has been found at  $Z = 40$  ( $\approx 5$  MeV) and it is predicted to decrease when going towards  $Z = 28$  [5].

The present work reports on the measurement of the excited states of the  $N = 50$   $^{83}\text{As}$ ,  $^{82}\text{Ge}$ , and  $^{81}\text{Ga}$  isotones. Since the wave functions of the states contain large cross-shell particle–hole excitation components with increasing excitation energy and spin, the corresponding excitation energies reflect the size of the shell gap. The comparison of the experimentally determined spectra with the predictions of detailed shell-model calculations is used to ascertain the size of the  $N = 50$  shell gap at  $Z = 28$ . Similar extrapolation methods have been used in the literature to probe the residual interaction and single-particle energies [7–10]. Recent mass measurements have allowed to extract the effective  $N = 50$  gap values up to  $Z = 31$  (Ga) [11], leaving the evolution of the shell towards  $Z = 28$  (Ni) still unknown. In this work, we show a method of determining, within the proposed model, the shell gap for the doubly-magic nucleus  $^{78}\text{Ni}$ , presently unreachable for most radioactive ion-beam facilities.

## 2. Experimental methods

Neutron-rich nuclei in the vicinity of  $^{78}\text{Ni}$  have been populated as products of multi-nucleon transfer reactions [12] following the collision of a  $^{82}\text{Se}$  beam onto  $^{238}\text{U}$  targets. The  $^{82}\text{Se}$  ions were accelerated to an energy of 515 MeV by the combination of the Tandem-XTU and the ALPI superconducting LINAC accelerators of the Legnaro National Laboratories (LNL). Two experiments were performed using isotopically enriched targets of  $^{238}\text{UO}_2$  and metallic  $^{238}\text{U}$  with the thickness of  $400 \mu\text{g}/\text{cm}^2$  and  $1000 \mu\text{g}/\text{cm}^2$ , respectively. Projectile-like nuclei were analyzed by the PRISMA magnetic spectrometer [13], placed at the reaction grazing angle of  $64^\circ$  with respect to the beam direction. Element identification ranging from  $Z = 24$  to  $Z = 43$  has been obtained from the energy loss measurement at the focal plane of the spectrometer. The average mass resolution achieved was about  $\Delta A/A = 1/180$  allowing a clean mass identification of all detected reaction products. The  $\gamma$  rays following the de-excitation of the reaction products were detected by the CLARA array [14], composed of 23 Compton-suppressed Ge Clover detectors, in coincidence with the projectile-like fragments detected by the PRISMA spectrometer. Doppler correction of the  $\gamma$  rays was performed on an event-by-event basis, taking the information of the recoil velocity vector determined by the reconstruction of the ion trajectories and the angle between this velocity vector and the direction of the  $\gamma$  ray emitted from the recoil. The energy resolution of the Doppler corrected  $\gamma$ -ray photopeaks was around 0.8%. Fig. 1 shows mass gated  $\gamma$ -ray spectra for the  $^{83}\text{As}$ ,  $^{82}\text{Ge}$ , and  $^{81}\text{Ga}$  isotones. Due to the limited acceptance of the PRISMA spectrometer as well as low efficiency of the CLARA array, coincidence data from the experiment was very limited. Therefore, coincidence information was obtained in a second experiment performed at LNL with the same reaction using the GASP  $4\pi$   $\gamma$ -ray spectrometer [15]. In this case, a thick  $^{238}\text{U}$  metallic target ( $60 \text{ mg}/\text{cm}^2$ ) was employed, in which all the reaction

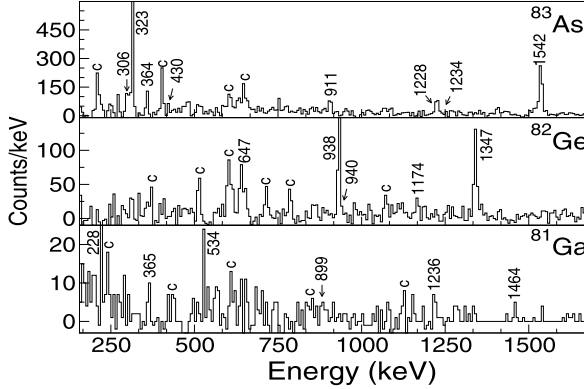


Fig. 1. Doppler-corrected  $\gamma$ -ray spectra for  $^{83}\text{As}$ ,  $^{82}\text{Ge}$  and  $^{81}\text{Ga}$  isotones after charge and mass selection. The “c” contamination lines present in the spectra are mainly due to the mass-leakage from the adjacent isotopes with mass (A-1). Random coincidences, arising from inelastic scattering, have been subtracted from the mass gated spectra.

products were stopped. Data was collected by acquiring triple  $\gamma$  coincidences and was analyzed using two- and three-dimensional matrices.

The spin assignments of excited states have been determined on the basis of the combined information coming from decay branchings, angular distributions of gamma rays for the CLARA–PRISMA data and ADO ( $\gamma$ -ray angular distribution from oriented nuclei) ratios [16] for the GASP data. The angular distributions,  $W(\theta_2)/W(\theta_1)$ , are analyzed by taking into account the  $W(\theta_1)$  and  $W(\theta_2)$  intensities of the  $\gamma$  transitions detected at different angles with respect to the entrance direction of the PRISMA spectrometer. In the data analysis, we have used a fixed value of  $\theta_1 = 98.8^\circ$  while the  $\theta_2$  values range from  $98.8^\circ$  to  $174.1^\circ$  which corresponds to the CLARA angles. The normalization factors due to the different energy dependence of the detector relative efficiencies were obtained with a  $^{152}\text{Eu}$  source. Due to the fact that ions populated in the reaction move at relativistic velocity about  $v/c = 10\%$ , it is necessary to apply an additional correction factor on the angular distributions [17,18]. The normalized angular distributions for each corresponding ring are fitted using the method of least squares to the angular distribution function [19,20]. Due to the lack of statistics, we have considered only the Legendre Polynomial of second degree in the fitting procedure. The determination of spins and multipolarities from the experimental angular-distribution coefficients requires knowledge of the substate population  $P_m(J)$  of a state  $J$ , which is approximated by a Gaussian distribution of  $m$ -states [21]. Here the width of the substate population is given with  $\sigma$  and determines the degree of the alignment of the state  $J$ . In the analysis of the experimental data  $\sigma/J$  has been treated as a parameter and has been determined experimentally from the known states in different Se isotopes as  $\sim 0.6$  for E2 stretched quadrupole transitions.

The ADO ratio is defined as:

$$R_{\text{ADO}} = \frac{I_{\gamma_1}[\text{at } 35^\circ(145^\circ) \text{ gated by } \gamma_2]}{I_{\gamma_1}[\text{at } 90^\circ \text{ gated by } \gamma_2]} \quad (1)$$

where  $I_{\gamma_1}$  corresponds to the  $\gamma$ -ray coincidence intensity at  $35^\circ$  ( $145^\circ$ ) and  $90^\circ$  obtained by setting gates on  $\gamma_2$  detected at any angle. The  $\gamma$ -ray intensities are corrected by the detection efficiency of the GASP array for each corresponding ring. Typical ADO ratios are centered at 1.2 and 0.8 for stretched quadrupole and stretched dipole transitions, respectively.

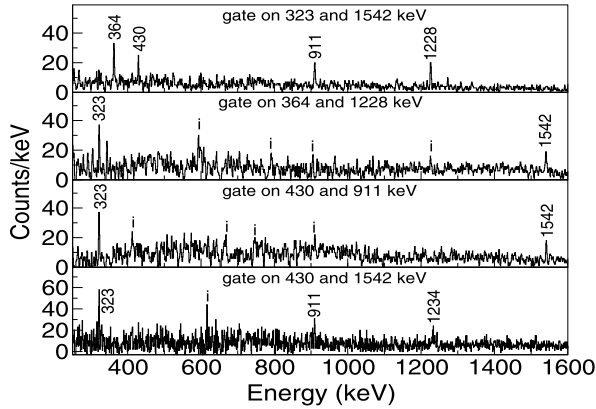


Fig. 2. Double-gated spectra obtained from the triple-coincidence data for  $^{83}\text{As}$  as in the thick-target experiment. The impurity lines marked with “i” are due to the reaction on residual oxygen contained into the target.

### 3. Experimental results

The collected statistics in the “thin-” and “thick-target” experiments has allowed to build level schemes for the  $^{83}\text{As}$ ,  $^{82}\text{Ge}$  and  $^{81}\text{Ga}$  nuclei. Preliminary results based only on the CLARA–PRISMA data of the present work have been reported in Refs. [22,23]. Previous knowledge on the excited states of the  $^{83}\text{As}$  nucleus mainly comes from  $\beta$ -decay studies [24,25] in which non-yrast states were mainly populated. Only 306- and 1542-keV  $\gamma$ -ray energies are known from Ref. [24] and a  $(3/2^-)$  assignment has been proposed for the 306-keV transition decaying to the ground state (g.s.) [25]. Among the transitions identified in the present work, we clearly observe the 306- and 1542-keV lines which decay directly to the g.s. In coincidence with the 1542-keV  $\gamma$  ray we find six new transitions, which can be divided in two branches on the basis of the coincidence relationships. A 323-keV line is found in coincidence with the 1542-keV transition as well as with the 1228-, 364-, 911-, and 430-keV transitions. The 430- and 911-keV lines, in mutual coincidence, are not observed in coincidence with the 1228- and 364-keV transitions defining two parallel branchings decaying to the state at 1.865 MeV which is de-excited by the 323-keV transition. The 430-keV line is also observed in coincidence with a 1234-keV transition decaying directly to the state at 1.542 MeV. All those transitions, supported by our preliminary identification of the present data [23] (except the 1234-keV one), have also been recently observed in a parallel work performed using a fusion–fission reaction [26]. Examples of coincidence relationships are shown in Fig. 2. The ground state spin–parity of  $^{83}\text{As}$  is not known experimentally and can be assigned either as  $3/2^-$  or  $5/2^-$ . However, the measured ground state spin–parity of its neighbouring nuclei at the  $N = 50$  isotonic chain,  $^{87}\text{Rb}$  ( $J^\pi = 3/2^-$ ),  $^{85}\text{Br}$  ( $J^\pi = 3/2^-$ ), and  $^{81}\text{Ga}$  ( $J^\pi = 5/2^-$ ), supports the expected inversion between the proton single-particle orbits  $1f_{5/2}$  and  $2p_{3/2}$  at  $N = 50$  indicating that the last unpaired proton remains in the  $2p_{3/2}$  orbit for  $Z > 34$  and in  $1f_{5/2}$  for  $Z < 34$ . We prefer, therefore, a  $(5/2^-)$  assignment for the g.s. of  $^{83}\text{As}$ . The angular distribution coefficient and ADO ratio for the 1542-keV transition decaying to the  $(5/2^-)$  g.s. suggest a quadrupole character, defining a new  $(9/2^-)$  level at 1.542 MeV. Those values for the 323-keV line support a dipole character of the transition identifying a new level at 1.865 MeV for which we suggest an  $(11/2)$  assignment, under the assumption of the increasing spin with the excitation energy consistent with the population of the yrast levels for those dissipative reactions. Based on the relatively large angular distribution coefficient as well as based

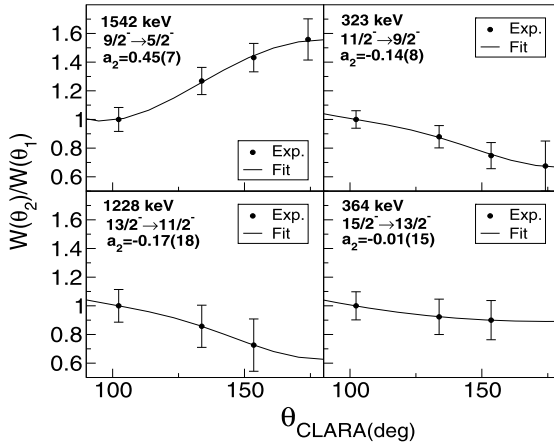


Fig. 3. Experimental angular distributions of  $\gamma$ -ray transitions in  $^{83}\text{As}$  measured in the thin-target experiment using the CLARA gamma array.

on systematics, we prefer a negative parity for this state. For the 1228- and 364-keV transitions observed above the  $(11/2^-)$  level, both angular distribution and ADO (Fig. 3) results favour a dipole character ( $\Delta = 1$ ) thus supporting  $(13/2^-)$  and  $(15/2^-)$  assignments for the corresponding levels at 3.093 and 3.457 MeV, respectively, under the same assumption of the increasing spin with the excitation energy. For the 430- and 911-keV transitions our data also support a dipole character identifying two states at 2.776 and 3.206 MeV, the former decaying to the  $(9/2^-)$  state at 1.542 MeV through a 1234-keV transition (see Fig. 3 and Table 1 for details).

The level scheme of  $^{82}\text{Ge}$  has been recently established from the  $\beta$ -n decay of  $^{83}\text{Ga}$  [27], spontaneous fission of both  $^{248}\text{Cm}$  [28] and  $^{252}\text{Cf}$  [29]. The 1347-, 938-, 940-, and 647-keV transitions with their proposed de-exciting states are reported in Ref. [28]. A 1174-keV transition has been observed in both Refs. [27,29] and its de-exciting state has been assigned as the second  $2^+$  state ( $2_2^+$ ) [29]. These observed states have been confirmed in this work. Using the  $\gamma\gamma$  coincidence data, the 1347-, 938-, and 940-keV transitions have been found in mutual coincidence. A 647-keV transition has been observed in coincidence only with the 1347- and 938-keV transitions while the 1174-keV line has been observed in coincidence only with the 1347-keV transition. Examples of the coincidence spectra are shown in Fig. 4. The ADO and angular distribution values for the 1347-, 938-, and 940-keV transitions support a quadrupole character suggesting  $2^+$ ,  $4^+$ , and  $6^+$  assignments for the states at 1.347, 2.285, and 3.225 MeV, respectively. For the 647-keV gamma ray, the ADO ratio supports a dipole character giving a  $I = 5$  assignment for the level 2.932 MeV, under the assumption of increasing spin with the excitation energy. The angular distribution coefficient for the 1174 keV  $\gamma$  line is compatible either with a stretched quadrupole or with a strongly mixed dipole transition. The level at 2.521 MeV has been reported in Ref. [29]. It decays to the  $2^+$  and to the g.s. through a 2525-keV line and it has been assigned as  $2_2^+$ . Therefore, we prefer a  $2^+$  assignment for this state (see Fig. 5 and Table 1 for details).

The g.s. spin-parity of  $^{81}\text{Ga}$  has been determined as  $5/2^-$  by the nuclear spin and magnetic moment measurements performed at ISOLDE [30]. Its non-yrast low-lying states are known from beta-decay studies [31,32] while very limited information on the yrast structure was previously known from the present CLARA-PRISMA data [22]. In this work we confirm the level observed

Table 1

$\gamma$ -ray energies ( $E_\gamma$ ), relative intensities ( $I_\gamma$ ), angular distribution coefficients ( $a_2$ ), and ADO ratios ( $R_{\text{ADO}}$ ), where possible, in  $^{83}\text{As}$ ,  $^{82}\text{Ge}$ , and  $^{81}\text{Ga}$ . The proposed spin–parity assignments for the levels involved as well as the excitation energies of initial ( $E_i$ ) and final ( $E_f$ ) states are also given.

$E_\gamma$ (keV) <sup>a</sup>	$I_\gamma$	$a_2$	$R_{\text{ADO}}$ <sup>b</sup>	$E_i \rightarrow E_f$ (keV)	$I_i^\pi \rightarrow I_f^\pi$
$^{83}\text{As}$					
306	16(6)	−0.7(9)		306 $\rightarrow$ 0	(3/2 <sup>−</sup> ) $\rightarrow$ (5/2 <sup>−</sup> )
323	54(8)	−0.14(6)	0.8(1)	1865 $\rightarrow$ 1542	(11/2 <sup>−</sup> ) $\rightarrow$ (9/2 <sup>−</sup> )
364	17(7)	−0.01(15)	0.7(1)	3457 $\rightarrow$ 3093	(15/2 <sup>−</sup> ) $\rightarrow$ (13/2 <sup>−</sup> )
430	13(3)	−0.08(16)	0.8(2)	3206 $\rightarrow$ 2776	
911	16(4)		0.8(1)	2776 $\rightarrow$ 1865	
1228	25(7)	−0.17(18)	0.8(1)	3093 $\rightarrow$ 1865	(13/2 <sup>−</sup> ) $\rightarrow$ (11/2 <sup>−</sup> )
1234	17(6)			2776 $\rightarrow$ 1542	
1542	100(9)	0.45(7)	1.2(1)	1542 $\rightarrow$ 0	(9/2 <sup>−</sup> ) $\rightarrow$ (5/2 <sup>−</sup> )
$^{82}\text{Ge}$					
647	22(7)		0.7(3)	2932 $\rightarrow$ 2285	5 <sup>+</sup> $\rightarrow$ 4 <sup>+</sup>
938	58(12)	0.37(15)	1.2(2)	2285 $\rightarrow$ 1347	4 <sup>+</sup> $\rightarrow$ 2 <sup>+</sup>
940	37(8)	0.48(16)	1.2(2)	3225 $\rightarrow$ 2285	6 <sup>+</sup> $\rightarrow$ 4 <sup>+</sup>
1174	19(6)	0.31(19)		2521 $\rightarrow$ 1347	(2 <sup>+</sup> ) $\rightarrow$ 2 <sup>+</sup>
1347	100(15)	0.34(14)	1.2(2)	1347 $\rightarrow$ 0	2 <sup>+</sup> $\rightarrow$ 0 <sup>+</sup>
$^{81}\text{Ga}$					
228	40(10)			(1464) $\rightarrow$ 1236	
365	35(10)			(2363) $\rightarrow$ (1998)	
534	38(14)			(1998) $\rightarrow$ (1464)	
899	35(13)			(2363) $\rightarrow$ (1464)	
1236	100(25)			1236 $\rightarrow$ 0	
1464	33(12)			(1464) $\rightarrow$ 0	

<sup>a</sup> Uncertainties are within 1 keV.

<sup>b</sup> ADO ratios are calculated for the thick target experiment.

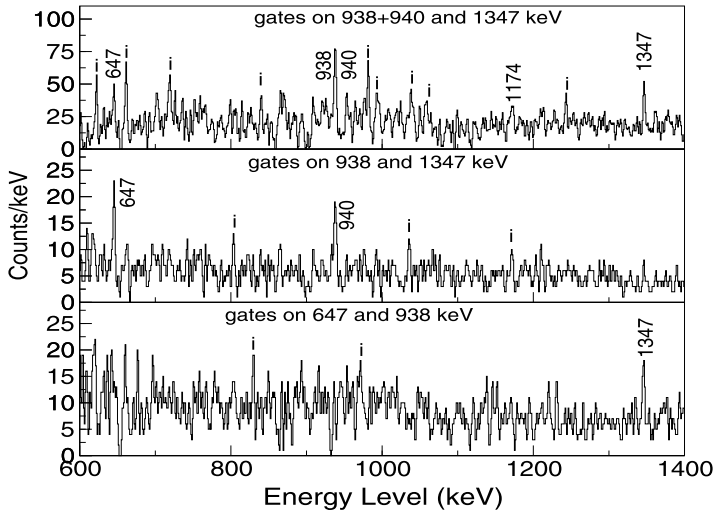


Fig. 4. Double-gated spectra obtained from the triple-coincidence data for  $^{82}\text{Ge}$  in the thick-target experiment. The impurity lines marked with “i” are due to the reaction on residual oxygen contained into the target.

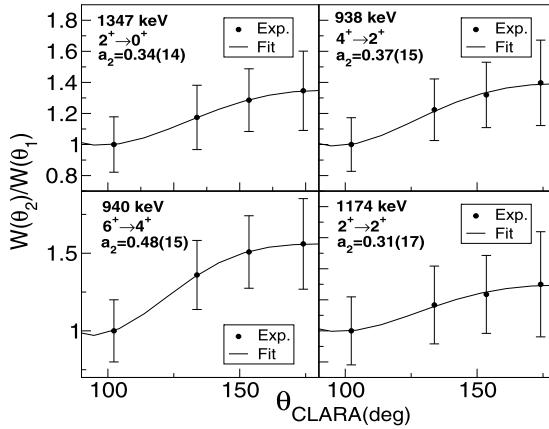


Fig. 5. Experimental angular distributions of  $\gamma$ -ray transitions in  $^{82}\text{Ge}$  measured in the thin-target experiment using the CLARA gamma array.

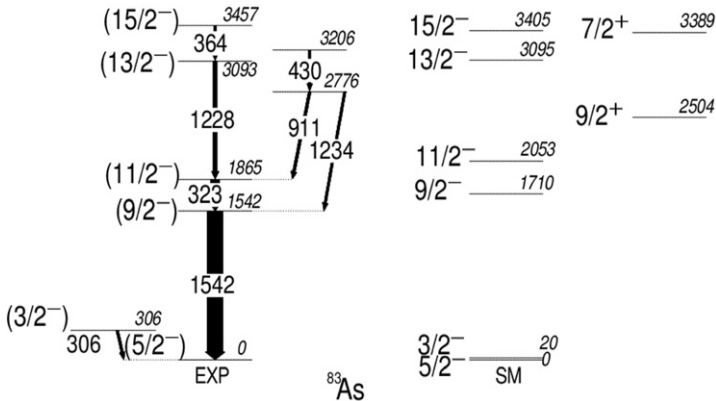


Fig. 6. Level scheme proposed for the  $^{83}\text{As}$  isotope as obtained from the present data. The experimental findings are compared with the results of shell-model calculations (see text).

at 1.236 MeV which directly decays to the g.s. [22] and we observe five new transitions which are tentatively arranged in the level scheme based on sum energies and branching ratios due to the very limited coincidence data for the 365-, 534-, and 1464-keV  $\gamma$  lines. On the basis of a  $5/2^-$  spin–parity assignment for the g.s. we prefer the  $(7/2^-)$  and  $(9/2^-)$  assignments for the levels at (1.236) and (1.464) MeV of excitation energy and  $(11/2^-)$  and  $(13/2^-)$  for the states observed at (1.998) and (2.363) MeV, respectively. The level schemes for the  $^{83}\text{As}$ ,  $^{82}\text{Ge}$ , and  $^{81}\text{Ga}$   $N = 50$  nuclei, are given in Figs. 6, 7, and 8, respectively. Table 1 shows the angular distribution coefficients and ADO ratios of the  $\gamma$ -ray energies of interest successively with the spin–parity assignments in the  $N = 50$  As, Ge, and Ga isotones.

#### 4. Shell-model calculations

The level structures in Figs. 6, 7, and 8 are compared with the results of shell-model calculations obtained using a combined effective interaction, based on the JJ4B residual interaction and



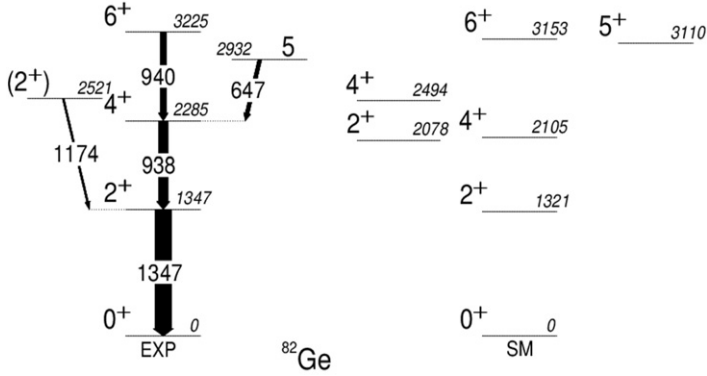


Fig. 7. Level scheme proposed for the  $^{82}\text{Ge}$  isotone as obtained from the present data. The experimental findings are compared with the results of shell-model calculations (see text).

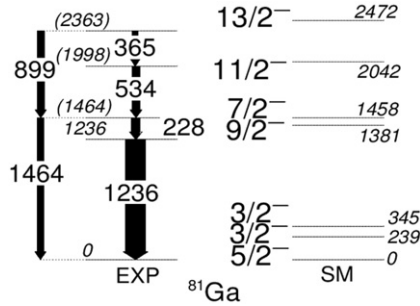


Fig. 8. Level scheme proposed for the  $^{81}\text{Ga}$  isotone as obtained from the present data. The experimental findings are compared with the results of shell-model calculations (see text).

on the two-body matrix elements of the Surface Delta Interaction (SDI) with a strength parameter of  $A = 0.2$  MeV.

The JJ4B effective interaction has been derived for the proton and neutron pfg configuration space built on the  $1f_{5/2}$ ,  $2p_{3/2}$ ,  $2p_{1/2}$  and  $1g_{9/2}$  single-particle orbits and it is an extended version of the JJ4APN interaction developed in order to reproduce the excited states of nuclei in the region of  $^{78}\text{Ni}$  [33,34]. The SDI has been adopted for the neutron sdg subspace built on the  $2d_{5/2}$ ,  $3s_{1/2}$  and  $1g_{7/2}$  orbits and for the cross-shell matrix elements between neutrons occupying the  $2d_{5/2}$ ,  $3s_{1/2}$  and  $1g_{7/2}$  and protons and neutrons occupying the  $1f_{5/2}$ ,  $2p_{3/2}$ ,  $2p_{1/2}$  and  $1g_{9/2}$  orbits. The values of the single-particle energies for the pfg space and for the sdg subspace are given in Table 2. The chosen configuration space assumes  $^{56}_{28}\text{Ni}_{28}$  as an inert core. To make the shell-model calculation feasible, the configuration space has been truncated by allowing two neutrons, at most, to be excited from the  $1g_{9/2}$  to the  $2d_{5/2}$ ,  $3s_{1/2}$  and  $1g_{7/2}$  orbits. The largest dimension of the model space encountered in this study for  $^{83}\text{As}$  exceeded 24 million (M-scheme). The shell-model code ANTOINE [35] has been used for diagonalization.

For  $^{83}\text{As}$  the calculated negative parity states compare reasonably well (in average within 200 keV of difference in energy) with the experimental ones. The order of the  $5/2^-$  and  $3/2^-$  levels is reproduced but the latter state is calculated only 20 keV above the ground state. Two positive parity states,  $9/2^+$  and  $7/2^+$  are predicted at 2.5 and 3.4 MeV of excitation energy, in qualitative

Table 2

Single-particle energies for the chosen model spaces (see text).

Model space	Single-particle energy (MeV)			
pfg for protons and neutrons	$E(1f_{5/2})$ −9.2859	$E(2p_{3/2})$ −9.6566	$E(2p_{1/2})$ −8.2695	$E(1g_{9/2})$ −5.8944
sdg for neutrons	$E(2d_{5/2})$ −1.1944	$E(3s_{1/2})$ −0.1680	$E(1g_{7/2})$ 0.2700	

agreement with the levels observed at 2.8 and 3.2 MeV and decaying to the  $(9/2^-)$  and  $(11/2^-)$  states through likely dipole transitions. In the case of  $^{82}\text{Ge}$  the predicted excitation energies compare well with the measured ones, the excitation energy differences being in average within 100 keV with somewhat larger deviations for the  $4^+$  and  $5^+$  states. The calculated  $4_2^+$  level is in agreement with the level observed at 2.521 MeV but we cannot exclude for it  $2^+$  assignment which is predicted at 2.078 MeV of excitation energy. The calculation compares also reasonably well with the tentative level scheme in the case of  $^{81}\text{Ga}$ . In Ref. [36] it has been suggested that based on systematic of the level schemes the low lying states of the odd-mass Ga nuclei could be described through the weak coupling between an unpaired valence proton and the neighboring even–even Zn “cores”. It is interesting to note that the excitation energy of the  $(9/2^-)$  state observed at 1.464 MeV matches quite well the  $2^+$  excitation energy of  $^{80}\text{Zn}$  of 1.492 MeV as expected for a configuration dominated by the weak coupling between the proton  $f_{5/2}$  and the corresponding core excitation. To compare the  $(7/2^-)$  state observed at 1.236 MeV with the systematic of the lighter Ga isotopes we have to refer to the  $(3/2^-)$  state. Here the excitation energy relative to the  $(3/2^-)$  level, identified in Ref. [31] at 351 keV is of 885 keV, in good agreement with the systematics (Fig. 14 in Ref. [36]). These results suggest also here a dominant configuration based on the weak coupling between the  $p_{3/2}$  state and the corresponding core excitations.

The calculated wave functions for states with medium and high spins show the presence of a significant component of the  $(\nu g_{9/2}^{-1} \otimes \nu d_{5/2}^1)$  configuration. As already observed in Ref. [37], for such states (above spin  $I = 4\hbar$  for  $^{82}\text{Ge}$  and  $I = (11/2)\hbar$  for  $^{83}\text{As}$ ), due to the contribution of particle–hole excitations across the gap, the excitation energies are very sensitive to the value of the neutron single-particle energies and therefore to the size of the  $N = 50$  energy gap at  $Z = 28$ . This value has been determined through a best fit procedure between the experimentally determined excited states of  $^{83}\text{As}$  and  $^{82}\text{Ge}$  and the calculated levels, using the  $(\nu E_{d_{5/2}} - \nu E_{g_{9/2}})$  energy difference as a parameter. The best agreement has been obtained for a gap size of 4.7(3) MeV, the error being determined through a standard deviation procedure. Fig. 9 shows the calculated single-particle levels reported as a function of the  $N = 50$  shell-gap value for  $^{82}\text{Ge}$ , and  $^{83}\text{As}$ . The flat behavior of the low-spin states up to  $4^+$  for  $^{82}\text{Ge}$  and  $(11/2^-)$  for  $^{83}\text{As}$  indicates a dominant proton character for such levels. Cross-shell components become more relevant for higher-spin states, i.e.  $5^+$  and  $6^+$  for  $^{82}\text{Ge}$  and  $(13/2^-)$  and  $(15/2^-)$  for  $^{83}\text{As}$ , leading to a strong dependence of the excitation energies on the gap size.

## 5. Discussion

It is interesting to compare the gap size deduced in the present work with the values obtained from experimental two neutron separation energies reported in Ref. [11]. The results of the atomic mass measurements (Fig. 4 of Ref. [11]) indicate a reduction of the effective shell gap

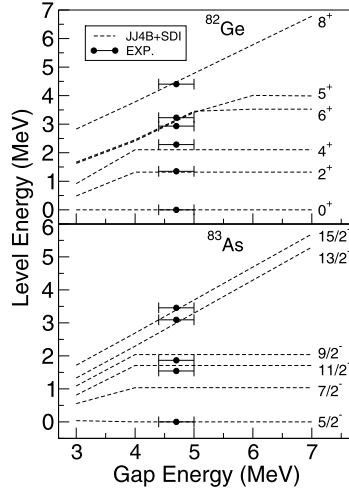


Fig. 9. Level energies of the  $^{82}\text{Ge}$  and  $^{83}\text{As}$  nuclei calculated, as described in the text, as a function of the  $N = 50$  shell gap energy. The best agreement with the experimental energies (indicated by full dots) is obtained for a gap value of 4.7(3) MeV.

down to Ge ( $Z = 32$ ), followed by an increase from Ga ( $Z = 31$ ). Notice that the experimental “shell gaps” given in Fig. 4 of Ref. [11] have to be considered as “effective shell gaps” since they include the monopole effects from valence nucleons. The gap size value of 4.7(3) MeV extracted from the present analysis confirms the increasing trend observed below  $Z = 32$  in accordance to the prediction of the Finite Range Droplet Mass formula among the mass models reported in Ref. [6] and excludes a weakening of the  $N = 50$  shell gap towards  $Z = 28$ . The observed minimum of the effective gap size at  $Z = 32$  [11] is also in agreement with the present analysis. Starting from a value of 4.7(3) MeV, a monopole contribution of  $-1.1$  MeV has been estimated by means of simple shell model considerations using the JJ4B two-body matrix elements. This means an effective gap value, which is valence-particle dependent, of 3.6 MeV at  $Z = 32$ , in qualitative agreement with the conclusion of Ref. [11]. Similarly, the recent large-scale shell-model calculations using proton  $pf$  and neutron  $fpgd$  shells explain the minimum of the  $N = 50$  gap at  $Z = 32$  and the following increase towards  $Z = 28$  indicating a robustness of the gap in  $^{78}\text{Ni}$  [10]. In the recent work of Porquet and Sorlin [38] the evolution of the  $N = 50$  gap is discussed. The trend determined from the two neutron separation energy shows a change of slope at  $N = 32$  attributed by the authors to the presence of extra correlations in the ground states. Using different extrapolation methods which include the excitation energy of the  $8^+$  states, instead of the  $0^+$  g.s., in the determination of the two neutron separation energies as well as one neutron separation energies, the authors predict an uncorrelated gap value for  $N = 50$  and  $Z = 28$  as 4.2 MeV. This value matches well with our result (uncorrelated gap value) of 4.7(3) MeV which does not indicate a substantial quenching of the  $N = 50$  shell gap at  $Z = 28$ .

## 6. Summary

In summary, the excited structures of the  $N = 50$  As, Ge, and Ga isotones have been investigated using multi-nucleon transfer reactions. New  $\gamma$  transitions have been identified for  $^{83}\text{As}$  and  $^{81}\text{Ga}$  and the level scheme of  $^{82}\text{Ge}$  has been confirmed. The  $N = 50$  shell gap at  $Z = 28$  has been

determined through the comparison of the excited states with the results of shell-model calculations. The result confirms the increasing trend of the effective gap below  $Z = 32$  and excludes the proposed quenching of the shell structure towards  $Z = 28$ .

## Acknowledgements

We thank O. Sorlin for the useful discussions and the accelerator crews of LNL for the excellent support. A.F.L. acknowledges partial support of this work from NSF grants PHY0244389 and PHY0555396. This work has been partially supported by the European Commission within the Sixth Framework Programme through I3-EURONS (contract No. RII3-CT-2004-506065) and the DGF (Germany under contract No. DE1516/-1).

## References

- [1] I. Hamamoto, et al., Nucl. Phys. A 683 (2001) 255.
- [2] T. Otsuka, et al., Prog. Theor. Phys. Suppl. 146 (2002) 6.
- [3] T. Otsuka, T. Suzuki, R. Fujimoto, H. Grawe, Y. Akaishi, Phys. Rev. Lett. 95 (2005) 232502, and references therein.
- [4] J. Dobaczewski, et al., Prog. Part. Nucl. Phys. 59 (2007) 432, and references therein.
- [5] O. Sorlin, M.-G. Porquet, Prog. Part. Nucl. Phys. 61 (2008) 602.
- [6] J.M. Pearson, et al., Nucl. Phys. A 777 (2006) 623.
- [7] H. Grawe, K. Langanke, G. Martinez-Pinedo, Rep. Prog. Phys. 70 (2007) 1525.
- [8] M.-G. Porquet, et al., Eur. Phys. J. A 40 (2009) 131.
- [9] K. Sieja, F. Nowacki, Phys. Rev. C 81 (2010) 061303(R).
- [10] K. Sieja, F. Nowacki, Phys. Rev. C 85 (2012) 051301(R).
- [11] J. Hakala, et al., Phys. Rev. Lett. 101 (2008) 052502.
- [12] R. Broda, J. Phys. G 32 (2006) R151.
- [13] A.M. Stefanini, et al., Nucl. Phys. A 701 (2002) 217c.
- [14] A. Gadea, et al., Eur. Phys. J. A 55 (2004) 193.
- [15] D. Bazzacco, in: Proceedings of the Intern. Conference on Nuclear Structure at High Angular Momentum, vol. II, Ottawa, 1992, Rep. No. AECL10613, p. 376.
- [16] M. Piiparinen, et al., Nucl. Phys. A 605 (1996) 191.
- [17] D. Montanari, et al., Phys. Lett. B 697 (2011) 288.
- [18] Olliver, T. Glasmacher, A.E. Stuchbery, Phys. Rev. C 68 (2003) 044312.
- [19] H. Ejiri, M.J.A. de Voigt, Gamma-Ray and Electron Spectroscopy in Nuclear Physics, Clarendon Press, Oxford, 1989.
- [20] E. Der Mateosian, A.W. Sunyar, Atomic Data and Nuclear Data Tables 13 (1974) 391.
- [21] T. Yamazaki, Nuclear Data A 3 (1967) 1.
- [22] G. de Angelis, Nucl. Phys. A 787 (2007) 74c.
- [23] E. Sahin, et al., AIP Conf. Proc. 1012 (2008) 139.
- [24] J.A. Winger, John C. Hill, F.K. Wohn, R.L. Gill, X. Ji, B.H. Wildenthal, Phys. Rev. C 38 (1988) 285.
- [25] D. Verney, et al., Braz. J. Phys. 34 (2004) 979.
- [26] M.-G. Porquet, et al., Phys. Rev. C 84 (2011) 054305.
- [27] J.A. Winger, et al., Phys. Rev. C 81 (2010) 044303.
- [28] T. Rząca-Urban, W. Urban, J.L. Durell, A.G. Smith, I. Ahmad, Phys. Rev. C 76 (2007) 027302.
- [29] J.K. Hwang, et al., Phys. Rev. C 84 (2011) 024305.
- [30] B. Cheal, et al., Phys. Rev. Lett. 104 (2010) 252502.
- [31] D. Verney, et al., Phys. Rev. C 76 (2007) 054312.
- [32] F. Ibrahim, et al., Nucl. Phys. A 787 (2007) 110c.
- [33] A.F. Lisetskiy, B.A. Brown, M. Horoi, H. Grawe, Phys. Rev. C 70 (2004) 044314.
- [34] J. Van de Walle, et al., Phys. Rev. Lett. 99 (2007) 142501.
- [35] E. Caurier, F. Nowacki, Acta Phys. Pol. B 30 (1999) 705.
- [36] I. Stefanescu, et al., Phys. Rev. C 79 (2009) 064302.
- [37] Y.H. Zhang, et al., Phys. Rev. C 70 (2004) 024301.
- [38] M.-G. Porquet, O. Sorlin, Phys. Rev. C 85 (2012) 014307.